Microscopic phase separation and ferromagnetic microdomains in Cr-doped Nd$_{0.5}$Ca$_{0.5}$MnO$_3$

S. Mori,[1] R. Shoji,[2] N. Yamamoto,[2] T. Asaka,[3] Y. Matsui,[3] A. Machida,[4] Y. Moritomo,[4] and T. Katsufuji[5]

[1]*Department of Materials Science, Osaka Prefecture University, Sakai-shi, Osaka 599-8531, Japan*
and Presto, JST, Japan
[2]*Department of Physics, Tokyo Institute of Technology, Tokyo 152-8551, Japan*
[3]*Advanced Materials Laboratory, NIMS, Tsukuba 305-0044, Japan*
[4]*Department of Applied Physics, Nagoya University, Nagoya 471-8601, Japan*
[5]*Department of Physics, Waseda University, Tokyo 169-8555, Japan*

We succeeded in observing ferromagnetic (FM) microdomains in the phase-separated state found in Cr-doped Nd$_{0.5}$Ca$_{0.5}$MnO$_3$ by low-temperature Lorentz microscopy. The presence of the FM microdomains with the size of 20–30 nm were found in Nd$_{0.5}$Ca$_{0.5}$Mn$_{1-y}$Cr$_y$O$_3$ for $y=0.03$. In addition, it is clearly shown that the low-temperature phase characterized as the phase-separated state consists of a fine mixture of the two competing ground states, the FM metallic state and the charge/orbital ordered insulator one. Our experimental findings clearly demonstrate the occurrence of microscopic and static phase separation in the Cr-doped manganites.

Immence resurgent activities on mixed-valent manganites reveal the importance of the existence of various-scale and real-space variation of physical properties and/or parameters.[1–6] Recently ferromagnetic resonance experiments have shown that two types of signals in ferromagnetic manganites are present, which was interpreted as evidence of electronic phase separation.[7] Furthermore, various experiments suggest the existence of magnetic polarons or mobile ferromagnetic clusters in manganites, which could be viewed as resulting from dynamic phase separation.[8] Recently Uehara *et al.* revealed in the transport and electron diffraction experiments that there coexist ferromagnetic (FM) metallic and so-called charge-exchange (CE)-type charge/orbital ordered (CO/OO) insulating domains, which was considered as static phase separation.[1] This coexistence of two distinct phases is responsible for colossal magnetoresistance (CMR) in low-T_c manganites. In addition, various theoretical models reveal the general tendency of static or dynamic phase separation.[4–6]

Recently, it was found that the long-ranged stable CO/OO state becomes a short-ranged one and the FM metallic state is induced by substituting Cr ions for the Mn ones in some doped manganites.[9–14] It is suggested that the low-temperature phase in the Cr-doped manganites such as Nd$_{0.5}$Ca$_{0.5}$Mn$_{1-y}$Cr$_y$O$_3$ with $0.01 < y < 0.05$ is characterized as a fine mixed phase of the FM metallic phase and the CO/OO insulator one.[9–12] Furthermore, these compounds show some unusual properties such as the so-called diffuse phase transition under the magnetic field, which is similar to the relaxor ferroelectrics.[15] These unusual properties found in the Cr-doped manganites could be regarded as resulting from the inhomogeneity in the electric, magnetic, and/or lattice systems.[10] The inhomogeneous state is characterized as the coexisting state consisting of different types of ordered states. Therefore, in order to understand some unusual properties in mangnites, it is important to elucidate the spatial distribution of some different phases characterizing the inhomogeneous state in the Cr-doped manganites at the microscopic scale.

In this work, we use electron microscopy and Lorentz microscopy to examine the spatial distribution of the CO/OO insulating phase and the FM metallic one in the phase-separated state. Here, we will demonstrate clearly the occurrence of static phase separation in Cr-doped manganites (Nd$_{0.5}$Ca$_{0.5}$Mn$_{1-y}$Cr$_y$O$_3$) by combining transmission electron microscopy with Lorentz microscopy. It is found that the FM microdomains with the size of 20–30 nm are embedded in the CO/OO insulating matrix.

High quality polycrystalline specimens of Nd$_{0.5}$Ca$_{0.5}$Mn$_{1-y}$Cr$_y$O$_3$ ($y=0.0$, 0.01, 0.03, and 0.05) were prepared with the standard solid-state reaction. The observation was carried out by using the Hitachi HF-3000F Lorentz electron microscopy equipped with the liquid-He cooling holder. No magnetic field was applied to the observed sample inside the electron microscopy. A microstructure related to the CO/OO phase was examined by obtaining the dark-field images taken by using the superlattice reflection spots due to the CO/OO structure.[12,13] On the other hand, the distribution of the FM domains was examined by the Fresnel imaging method in the Lorentz microscopy. The principle of the Fresnel imaging method has been reviewed in detail.[16,17] The physical properties such as magnetization and resistivity in the samples we used in this work have been reported.[12,13]

As already reported in Ref. 12, the Cr substitution for the Mn sites in Nd$_{0.5}$Ca$_{0.5}$MnO$_3$ destroyed the stable CE-type CO/OO structure and induced the FM phase. The low-temperature phase in the Nd$_{0.5}$Ca$_{0.5}$Mn$_{0.95}$Cr$_{0.05}$O$_3$ compound is characterized as the FM metallic phase.[12] First of all, the magnetic domain structure in the FM metallic phase of Nd$_{0.5}$Ca$_{0.5}$Mn$_{0.95}$Cr$_{0.05}$O$_3$ was investigated by the Fresnel imaging method. It should be noticed that in the Fresnel image, magnetic domain boundaries give rise to characteristic alter-
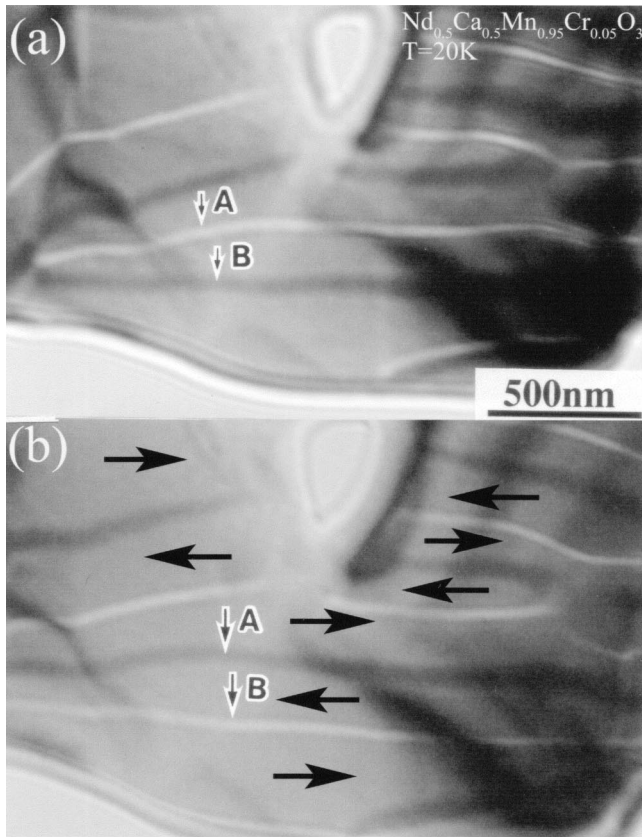
FIG. 1. Magnetic domain structure in the FM metallic phase of $Nd_{0.5}Ca_{0.5}Mn_{0.95}Cr_{0.05}O_3$ taken at 20 K. The Lorentz (Fresnel) images are obtained with the defocused value of (a) $+1.0$ mm (overfocused) and (b) -1.0 mm (underfocused), respectively. Arrows in (b) show the directions of the magnetic moment in each FM domain. Arrows (A) and (B) show the FM domain boundaries, respectively.

nating dark and bright contrast. Figures 1(a) and (b) show typical FM domain structure obtained at 20 K in $Nd_{0.5}Ca_{0.5}Mn_{0.95}Cr_{0.05}O_3$. These images were taken under overfocused and underfocused conditions, respectively. Note that the defocused value is about 1 mm. As shown in Figs. 1(a) and (b), the alternating arrangement of characteristic dark and bright line contrast due to the magnetic domain boundaries can be seen clearly. It can be understood that the arrangement of the dark and bright contrast is completely reversed by comparing Fig. 1(a) with Fig. 1(b). This indicates that FM domain boundaries give rise to the alternating arrangement of dark and bright line contrast. From careful analysis of the contrast in Fig. 1, the direction of the magnetic moment in each FM domains can be determined. The directions of the magnetic moment in each FM domains are depicted schematically in Fig. 1(b).

By using both the dark-field imaging method and the Fresnel imaging one, we investigated the spatial distribution of the CO/OO phase and the FM phase in the phase-separated region found in $Nd_{0.5}Ca_{0.5}Mn_{1-y}Cr_yO_3$ with $y = 0.03$. Figure 2(a) shows microstructure related to the CO/OO phase at 20 K, which is taken by using the superlattice spots due to the charge/orbital ordering. As already re-
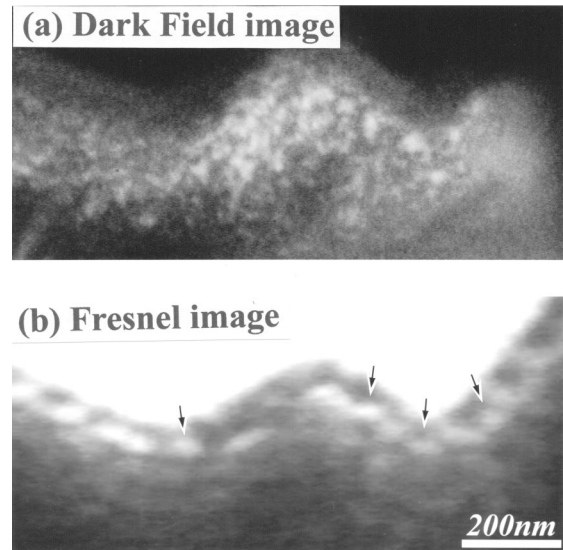

FIG. 2. (a) Dark-field image taken by using the superlattice spot due to the CO/OO structure in $Nd_{0.5}Ca_{0.5}Mn_{0.97}Cr_{0.03}O_3$. In the dark-field image, the regions with bright contrast are identified as the CO/OO phase. (b) Fresnel image in $Nd_{0.5}Ca_{0.5}Mn_{0.97}Cr_{0.03}O_3$. Characteristic circle-shaped contrast due to the FM domains can be clearly seen. The images (a) and (b) are taken at 20 K in the same area, respectively.

ported in our previous work,[12,13] the CO/OO phase exists as the microdomains with the size of 20–30 nm in the phase-separated state. On the other hand, Fig. 2(b) is a Fresnel image showing the presence of the FM microdomains with the size of 20–30 nm. Note that Fig. 2(b) is taken at 20 K in the same area as Fig. 2(a). The regions with circle-shaped contrast, indicated by arrows in Fig. 2(b), correspond to the FM microdomains. By comparing the images shown in Figs. 2(a) and (b), two different phases, the CO/OO phase and the FM one, coexist as the microdomains with the size of 20–30 nm. That is, the phase-separated state in the $Nd_{0.5}Ca_{0.5}Mn_{0.97}Cr_{0.03}O_3$ compound is characterized as fine mixture of the two different phases with the 20–30-nm size.
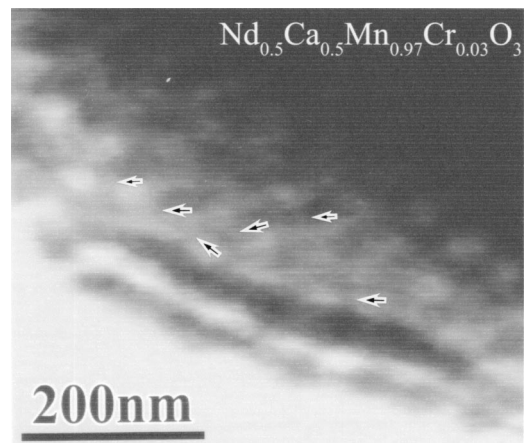

FIG. 3. (a) Fresnel image at 20 K in $Nd_{0.5}Ca_{0.5}Mn_{0.97}Cr_{0.03}O_3$, together with the directions of the magnetic moment in the FM domains (arrows).

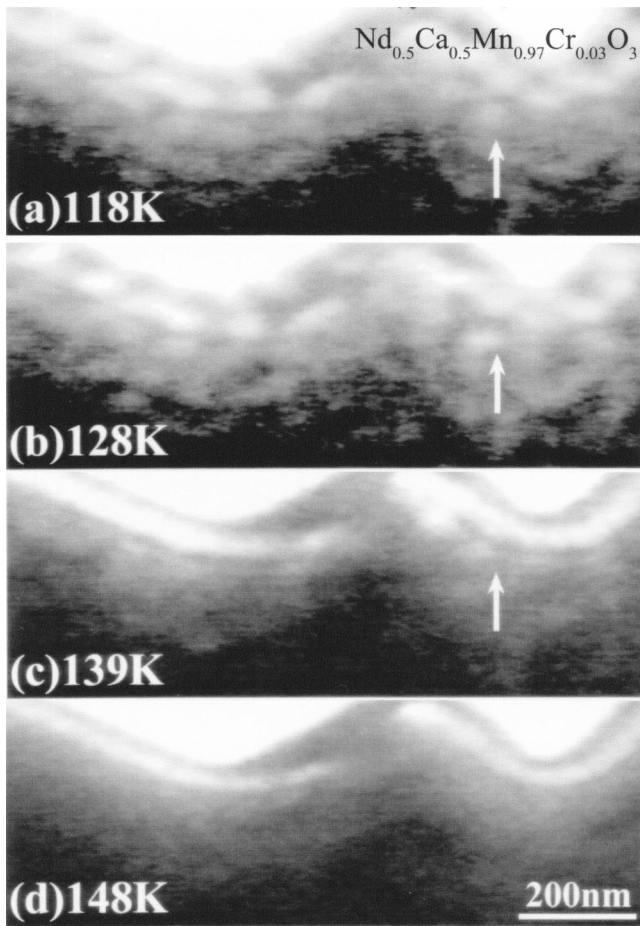FIG. 4. Change in the FM domain structure on warming in $Nd_{0.5}Ca_{0.5}Mn_{0.97}Cr_{0.03}O_3$. The images are taken at (a) 118 K, (b) 128 K, (c) 139 K, and (d) 148 K, respectively. Note that the circle-shaped contrast due to the FM microdomains indicated by a white arrow becomes weaker on warming.

This finely mixed state should be regarded as microscopically phase-separated state. In addition, we analyzed carefully the characteristic circle-shaped contrast, in order to de-termine the direction of the magnetic moment in the FM microdomains found in the phase-separated state. Figure 3 shows the Fresnel image showing the presence of the FM microdomains in $Nd_{0.5}Ca_{0.5}Mn_{0.97}Cr_{0.03}O_3$. The directions of the magnetic moment are also indicated by arrows in Fig. 3. It should be noticed that the directions of the magnetic moment in the FM microdomains are determined approximately from the analysis of the circle-shaped dark-and-bright contrast.

Figure 4 shows change in the microstructure related to the FM microdomains on warming from 120 K, which is below the FM transition temperature of $T_c = 140$ K. Figures 4(a) and (b) are, respectively, taken at 118 and 128 K, whose temperatures are below $T_c = 140$ K. In Figs. 4(a) and (b), the FM microdomains with the size of 20–30 nm can be seen clearly. On warming the sample to the FM transition temperature, the characteristic contrast due to the FM micro-domains becomes weaker, as shown in Fig. 4(c) at 139 K. On further warming, the characteristic contrast disappear, as evident in Fig. 4(d) at 148 K. This indicates clearly that the regions with the characteristic circle-shaped dark-and-bright contrast correspond to the FM microdomains in the Fresnel image shown in both Figs. 2(b) and 3.

In summary, the presence of the FM microdomains with the 20–30-nm size is clearly demonstrated in the Fresnel imaging method. In addition, it is found that the low-temperature phase in $Nd_{0.5}Ca_{0.5}Mn_{1-y}Cr_yO_3$ with $y = 0.03$ is characterized as fine mixed state of two competing ground state, the CO/OO insulator state and the FM metallic one. This means that microscopic and static phase separation takes place at the low temperature below 140 K in $Nd_{0.5}Ca_{0.5}Mn_{1-y}Cr_yO_3$ with $y = 0.03$. This inhomogeneous state should play a crucial role in the unusual properties such as the diffuse phase transition and the CMR effect found in the Cr-doped manganites.[14,15]

[1] M. Uehara, S. Mori, C. H. Chen, and S.-W. Cheong, Nature (London) **399**, 560 (1999).

[2] S. Mori, C. H. Chen, and S. W. Cheong, Phys. Rev. Lett. **81**, 3972 (1998).

[3] M. Fath, S. Freisem, A. A. Menovsky, Y. Tomioka, J. Asrts, and J. A. Mydosh, Science **285**, 1540 (1999).

[4] A. Moreo, S. Yunoki, and E. Dagotto, Science **283**, 2034 (1999).

[5] E. Dagotto, T. Hotta, and A. Moreo, Phys. Rep. **344**, 1 (2001).

[6] J. Burgy, M. Mayr, V. Martin-Mayor, A. Moreo, and E. Dagotto, Phys. Rev. Lett. **87**, 277202 (2001).

[7] M. M. Savosta and P. Novak, Phys. Rev. Lett. **87**, 137204 (2001).

[8] R. H. Heffner et al., Phys. Rev. Lett. **85**, 3285 (2000).

[9] T. Katsufuji, S. W. Cheong, S. Mori, and C. H. Chen, J. Phys. Soc. Jpn. **68**, 1090 (1999).

[10] Y. Moritomo, A. Machida, S. Mori, N. Yamamoto, and A. Naka-mura, Phys. Rev. B **60**, 9220 (1999).

[11] A. Machida, Y. Moritomo, E. Nishibori, N. Takata, M. Sakata, K. Ohoyama, S. Mori, N. Yamamoto, and A. Nakamura, J. Phys. Soc. Jpn. **69**, 3536 (2000).

[12] R. Shoji, S. Mori, N. Yamamoto, A. Machida, Y. Moritomo, and T. Katsufuji, J. Phys. Soc. Jpn. **70**, 267 (2001).

[13] S. Mori, R. Shoji, N. Yamamoto, A. Machida, Y. Moritomo, and T. Katsufuji, J. Phys. Soc. Jpn. **71**, 1280 (2002).

[14] A. Barnabe, A. Maignan, M. Hervieu, F. Demay, C. Martin, and B. Raveau, Appl. Phys. Lett. **71**, 3907 (1997).

[15] T. Kimura, R. Kumai, Y. Okimoto, Y. Tomioka, and Y. Tokura, Phys. Rev. B **62**, 15 021 (2000).

[16] L. Reimer, *Transmission Electron Microscopy, Physics of Image Formation and Microanalysis* (Springer-Verlag, Berlin, 1984).

[17] S. Mori, T. Asaka, and Y. Matsui, J. Electron Microsc. **51**, 225 (2002).